ASSESSMENT OF SEISMIC AND INFRASOUND SIGNALS IN KOREA WITH GROUND TRUTH

Brian Stump[1], Myung-Soon Jun[2], Chris Hayward[1], Jeong-Soo Jeon[2], Il-Young Che[2], Sara Mihan House[1], and Tae-Sung Kim[1]

Southern Methodist University[1]
Korea Institute of Geosciences and Mineral Resources[2]

Sponsored by Defense Threat Reduction Agency

Contract No. DSWA01-98-C-0131

ABSTRACT

A four-element, 1-km aperture seismo-acoustic array is being operated northeast of Seoul, Korea. Each element of the array consists of a GS-13 vertical seismometer (1 Hz) in a shallow borehole (~10 m) and a low-frequency acoustic gauge connected to an 11-element hose array (7.6 m hoses) at the surface. The array is being used to assess the importance of co-located seismic and acoustic sensors for the purposes of: (1) quantifying wind as a source of seismic and acoustic noise; (2) constraining propagation path effects in the atmosphere and solid earth; (3) locating the sources of the waves; (4) characterizing the source type. Combined analysis of the seismic and acoustic data can be particularly important in identifying sources of industrial blasting. Seismic noise estimates illustrate a level that is only slightly above the low noise model on average. Acoustic noise levels resolve the microbaroms during low noise times but document a nearly 50 dB increase in noise during the windiest periods. Infrasonic noise in the 0.01 to 5 Hz band increases rapidly with wind velocity. The seismic noise shows little or no dependence on wind velocity. Analysis of the data suggests that there are many more acoustic signals than seismic (4-10 times). The majority of the acoustic signals occurs during working hours and are constrained to several narrow azimuth ranges. These observations suggest that the signals are man made. Approximately 1/4 of all seismic signals are associated with an acoustic arrival. The seismo-acoustic observations come from sources in the 30 to 200 km range and occur during working hours, local time. The 30 to 200 km observation distance is surprising in that average atmospheric velocity models predict no acoustic returns in this range. Average atmospheric models modified by meteorological data for the troposphere indicate the possibility of ducting in the troposphere as an explanation for these arrivals. Event location is based upon regional seismic phase identification (P_n, P_g, P_mP, L_g, R_g) using the array and back azimuth estimates from both the seismic and acoustic data. Aliasing for the short wavelength infrasound signals is reduced using broadband back azimuth estimates. Additional infrasound sensors with 100 m offset are planned to further reduce the aliasing problem. Many of the infrasound signals have good signal to noise from 1 to beyond 4 Hz. Despite the small size of the array, event clusters are identified at regional distances. Waveform comparisons of these clusters suggest that the events are from common source areas. The high Q path of the Korean Peninsula results in regional seismograms that have significant energy to frequencies as high as 16 Hz, the corner frequency for the anti-alias filters. Events associated with acoustic signals are presumed to be from mining regions. Ground truth in the form of in-mine observations provides validation of this interpretation. These data are also used to assess blasting practices and their relationship to the observed seismic and infrasound signals. The existence of Rg arrivals and dominance of P energy at high frequency are consistent with this interpretation. There is more event-to-event variation in the acoustic signals than the sesmic signals within the event groups, suggesting the effect of variable atmospheric propagation effects consistent with ray paths in the troposphere.

KEY WORDS: Seismo-acoustic, mining, discrimination, infrasound

OBJECTIVE

The Korean Peninsula (Figure 1) provides a unique laboratory for studying regional seismic wave propagation. Numerous broadband seismic stations in the region and a variety of natural and man-made sources provide opportunities for characterizing wave propagation and source effects within the region. The region includes two

seismic arrays, KSRS and CHNAR, the seismo-acoustic array near Chulwon operated by Korea Institute of Geosciences and Mineral Resources (KIGAM) and Southern Methodist University (SMU). Figure 1 illustrates the seismicity of the region using preliminary event locations made in this study as well as event locations by others.

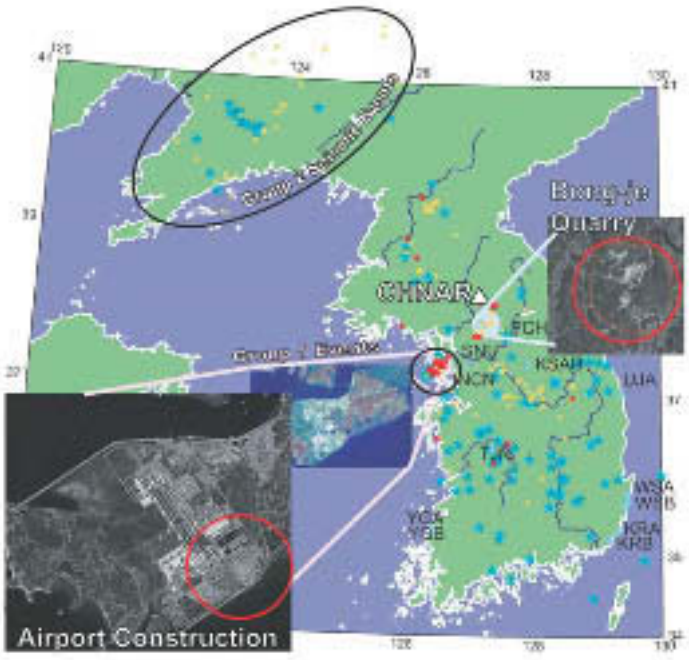

Figure 1. The map shows the events located on the basis of two months of CHNAR data. Seismo-acoustic events are shown as solid red dots; seismic events without acoustic signals are shown as yellow dots; events from the Korean NDC bulletin are marked as blue stars; and ground-truth studies based on event locations are highlighted as solid pink and blue circles. The broadband stations, the existing seismo-acoustic research array CHNAR, and the IMS array KSAR are light blue triangles. The inset images are taken from Landsat-7 satellite imagery and show two of the verified sources. (adapted from Stump *et al.*, 2000)

Intra-plate earthquakes are observed in and around the Korean Peninsula (Jun, 1991; Jun and Kulhanek, 1991; Kim, 1980). Focal mechanisms for 22 of the largest events in the last century (Jun *et al., 1999)* show predominantly strike-slip faulting with a small amount of thrust. The average compressional axis trends ENE to WSW across the entire Peninsula , which suggests the peninsula, is a single tectonic region and possibly single seismic structure. In NE China, the Tan-Lu fault is a particularly active source region. This left-lateral fault system may have originated the 1975 Haicheng earthquake. The peninsula also has an active mining industry. Near-surface mining explosions generate regionally observed seismic and acoustic signals (Hagerty *et al.,* 1999). Sorrels, Herrin and Bonner (1997) have used such acoustic signals recorded at TXAR to identify mining explosions in southwestern New Mexico.

RESEARCH ACCOMPLISHED

In the last year, the work has focused on four areas: (1) Quantifying wind as a source of seismic and acoustic noise; (2) Constraining propagation path effects in the atmosphere and earth; (3) Determining event origins; (4) Characterizing source types. The following discussion is organized into these four areas.

Quantification of Wind as a Source of Seismic and Acoustic Noise

Seismic and infrasound noise analysis was undertaken for a twenty-day period (Day 30-49, 2000) during which the sites were snow covered. The purpose was to quantify the absolute seismic and acoustic noise levels at the array elements, the variation of each with local winds, and the relationship between seismic and acoustic noise.

Infrasound

The infrasound noise estimates for a representative array element (CHN00) are given in Figure 2 (left). Microbaroms show as a noise peak between 4 and 8 s. The effect of wind on spectral noise levels is shown in Figure 2 (right). Wind speed is measured10 m above ground at the array hub (CHN00). Below 4 Hz, noise levels increase with winds in excess of 1-2 m/s. Hedlin *et al*., 1999, have reported similar effects.

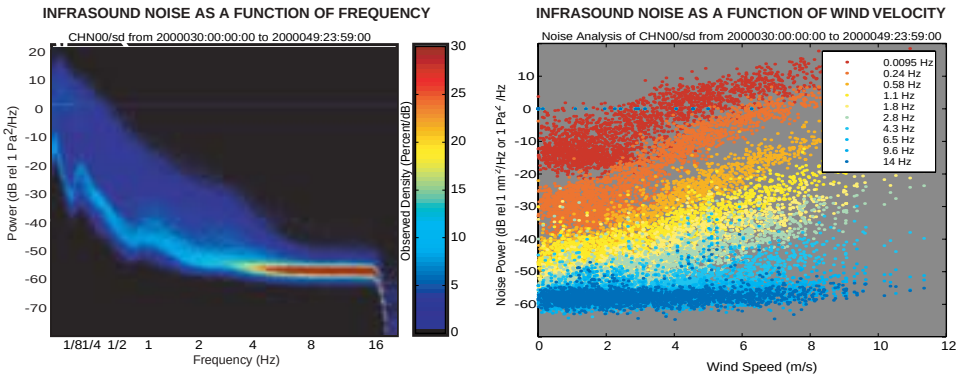

Figure 2: The power-normalized probability density as a function of frequency of 20 days of infrasound noise at CHN00 is plotted to the left. Noise power as a function of wind speed for different narrow band frequencies are plotted to the right.

Seismic

The same methodology was used to investigate wind generated seismic noise. Representative seismic noise plots superimposed on the low and high seismic noise models are reproduced in Figure 3. Although some time periods approach the low noise model levels, the most probable level is at least 10 dB higher, still well below the high noise model.

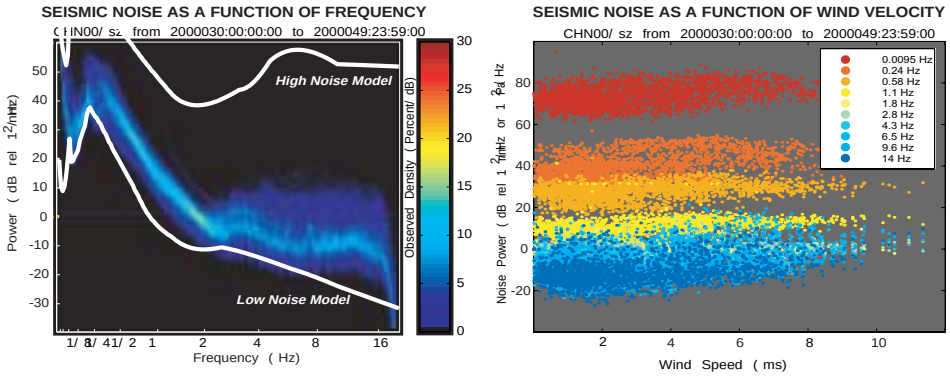

Figure 3: The power normalized probability density for 20 days of seismic noise at CHN00 is plotted as a function of frequency to the left. Noise values for different center frequencies are plotted as a function of wind speed to the right.

The low observed seismic noise is consistent with the borehole seismometer installation in competent rock. The seismic noise to wind velocity dependence is further illustrated in Figure 3 (right). Like the infrasound noise, for any one frequency band the seismic noise varies by 20 dB or less. There is little correlation between seismic noise and wind speed, thus this 20 dB is the controlling factor in the total seismic noise estimates. The lack of noise-wind correlation is consistent with the 10 m borehole and the low coupling the atmospheric pressure variations to seismic coupling in the site s hard rock. The peak in the seismic noise at 5s (Figure 3), the microseisms, occurs at nearly the same frequency as that in the infrasound data, the microbaroms (Figure 2). The similar peak period is consistent with a common cause for low frequency seismic and infrasound noise as suggested by Donn and Posmentier (1967)

Constraining Propagation Path Effects in the Atmosphere and Solid Earth

Seismic

Wave propagation characteristics across the Korean Peninsula must be quantified to interpret the seismograms recorded at CHNAR. Fortunately, there are many seismographs on the Peninsula including KIGAM s broadband network (Figure 1) and the IMS array KSRS. Data from these stations for a preliminary event set (Table 1 and Figure 4) was obtained to constrain estimates of propagation path effects.

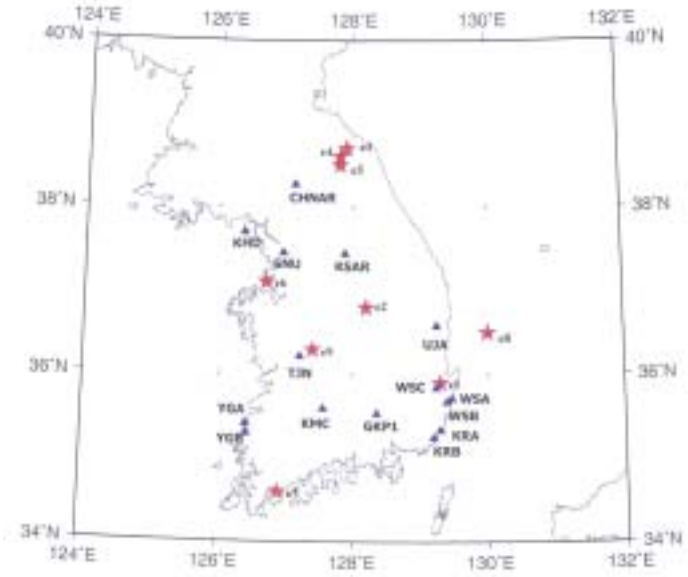

Figure 4: The map shows events (red stars) and seismic stations (blue diamonds) that were used in the preliminary wave propagation effects and source effects study.

Table 1. The table shows origin time and magnitude of 9 events located by KMA (Korea Meteorological Administration) and used to select a seismograms from stations on the Korean Peninsula.

Event No.	Origin time(GMT)		Location (Degree)		Mag.	Focal Depth (km)
	Mon-Day-Year	Hour-Min-Sec	Lat.	Lon.		
E1	9-11-99	20-56-53.0	35.9	129.3	3.2	5.9
E2	12-27-99	03-29-19.9	36.8	128.2	3.0	3.45
E3	01-18-00	06-08-49.5	38.7	127.9	3.0	14.3 ?
E4	05-11-00	06-01-08.4	38.6	127.8	2.9	0
E5	07-23-00	22-00-00.1	38.5	127.8	3.0	0
E6	10-27-00	22-10-11.8	37.1	126.7	2.7	Sea
E7	12-02-00	07-53-40.0	34.6	126.9	3.1	?
E8	12-09-00	09-51-00.0	36.5	130.0	3.7	Sea
E9	12-21-00	23-19-38.5	36.3	127.4	2.7	?

Figure 4 summarizes the event locations for events in Table 1 and shows the location of regional seismic stations. Events 1-2 and 7-8 are associated with earthquakes recognized by the KMA. Based upon associated infrasound signals at CHNAR, events 3-5 are explosions. This event set provides an opportunity to study both wave propagation through the peninsula and waveform characteristics associated with particular source types. As an example, consider the unfiltered record section from event 7 (Figure 5). At nearest stations P_g is the first arrival; beyond 150 km P_n is first. The largest phase associated with this earthquake is L_g. A R_g phase can be identified at stations less than 200 km from shallow events. At about 100 km, PmP is a strong phase. Such data provides important constraints upon regional propagation models. Figure 5 illustrates that modest magnitude (3.1) earthquakes can provide significant waveform data for constraining these models.

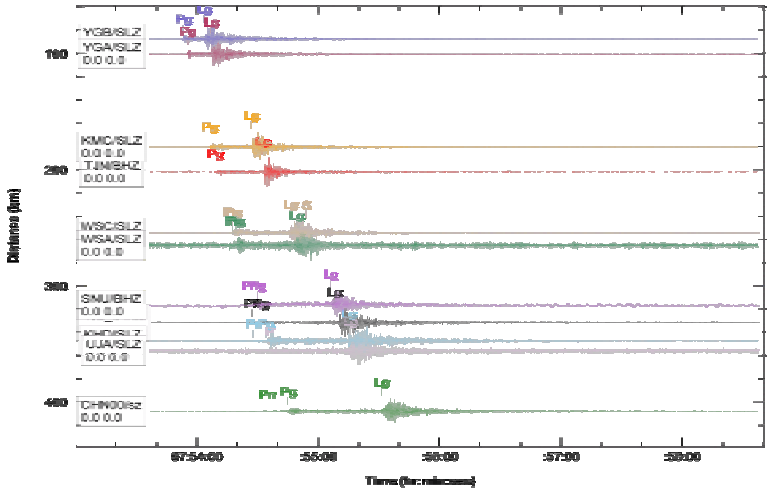

Figure 5: A record section shows waveforms from the stations from the KIGAM broadband network for Event 7 (Table 1 and Figure 4).

Infrasound

Stump et al.(2000) found that approximately one quarter of all seismic events recorded at CHNAR have associated infrasound signals. These events are attributed to mining explosions. At CHNAR they observed an average of three to four seismic events and one seismo-acoustic event per day. Analysis of the acoustic data suggested that there were many more acoustic signals than seismic. This observation motivated a more in depth analysis of the acoustic data at CHNAR in hopes of building a database useful for studying acoustic wave propagation effects. Seven days of CHNAR acoustic data were analyzed for each of October, November, February, April, June and August. Figure 6 summarizes the approach azimuth and time of day of these signals as determined by processing the array data.

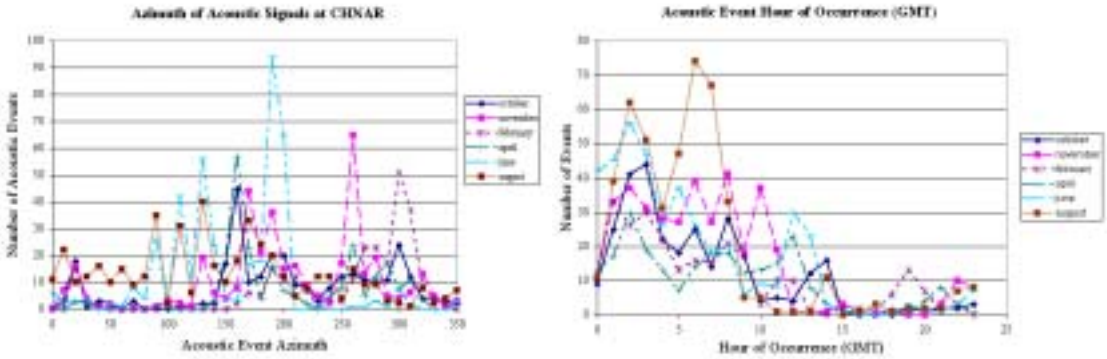

Figure 6: The azimuth of acoustic events from CHNAR as a function of month of year is displayed to the left. One-week periods of data from the months of October, November, February, April, June and August were analyzed. The hour (GMT) at which each of the events occurred is displayed to the right.

An average of nearly 50 coherent acoustic signals per day was observed on the CHNAR array, ten times more than the number of coherent seismic signals. Figure 6 (left), illustrates that the acoustic signals observed at CHNAR come from distinct azimuths that vary with month, possibly reflecting changes in regional wind patterns. For example, a large number of signals were observed between 80 and 140 degrees during June and August but not other months. These events are probably man made since they occur during normal work hours (Figure 6 right).

Locating the Sources of the Waves

Seismic

The network seismic data for the analyzed events (Table 1 and Figure 4) provide an initial resource to develop empirical travel time curves for the Korean Peninsula. Such curves may then be compared to complementary work (Lee, 1979; Kim et al., 1983; Kim et al., 1985; Kim, 1995; Kim et al., 1997; Kim et al., 1998a; Kim et al, 1998b). Using this data in a complete waveform modeling exercise will more fully resolve the distance and source contributions effects in observations. As a first step to understand the propagation in Korea, arrival time picks of all regional phases were made using the KMA event locations. The velocities of P_n, P_g, L_g phase were calculated as 8.2 km/sec, 6.6 km/sec, and 3.8 km/sec (Figure 7) respectively with individual arrival time errors as large as 5-10 s.

Event locations reported in Stump et al., 2000 used the simple relationship distance $X= (t_{Lg} - t_p)$ Æ 8 to produce single array locations from L_g-P time and back azimuth estimates from CHNAR. The data reproduced in Figure 7 suggests that for distances shorter than the P_g to P_n crossover, 155 km, that the simple distance estimate is $X_{<155} = (t_{Lg} - t_{Pg})$ Æ 8.9 and that beyond the crossover distance the simple estimate is $X_{>155} (t_{Lg} - t_{Pn})$ Æ 7.1. As Figure 5 illustrates, P_n is an emergent arrival that is over shadowed by P_g and so for small magnitude events care must be taken that P_n is indeed the identified first arrival used for estimating distance. For single array locations phase velocity measurements from the array can confirm phase identity.

Infrasound

Most seismo-acoustic signals (Figure 1) are 30 to 200 km from the array. These locations are based upon the seismic data and its association with an infrasound arrival (Stump et al., 2000). Locating acoustic-only signals requires an atmospheric velocity model. The first approach is to use an Effective Sound Velocity Structure (ESVS) based upon average seasonal variations in winds. Such a model predicts that between 30 to 200 km from the source, there will be no arrivals.

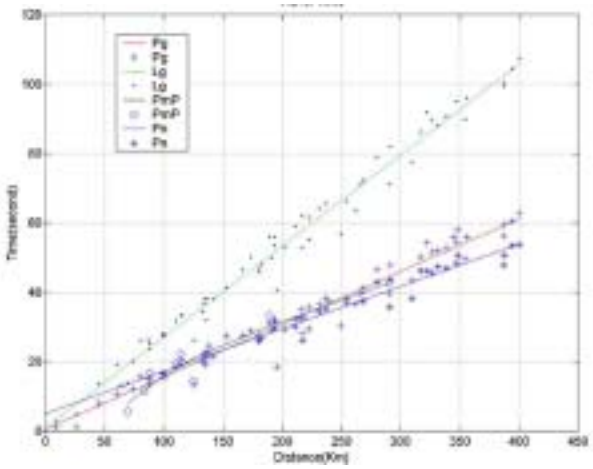

Figure 7: The figure shows arrival time data from the nine events in Table 1 based upon the KMA locations and the estimated travel time for each of the individual phases. A linear least square fit has been made to the picks.

At CHNAR, all observed seismo-acoustic signals fall within this theoretical blind zone. Arrivals in this range can be produced by tropospheric wind generated turning rays (Garc s et al ., 1998). Hagerty et al. (1999) attribute a troposphere duct to the infrasound first arrival from Kazakhstan mining explosions 250 km away. They also report that seasonal variations in troposphere winds lead to significant variations in the signal detectability. Che et al. (2000) have compared acoustic propagation in Korea based a seasonally averaged ESVS and a model with a troposphere based on regional meteorological observations. The seasonally averaged ESVS for October predicts no arrivals out to 220 km for paths traveling from S80W and only a single, low atmospheric arrival at close range from N80E.

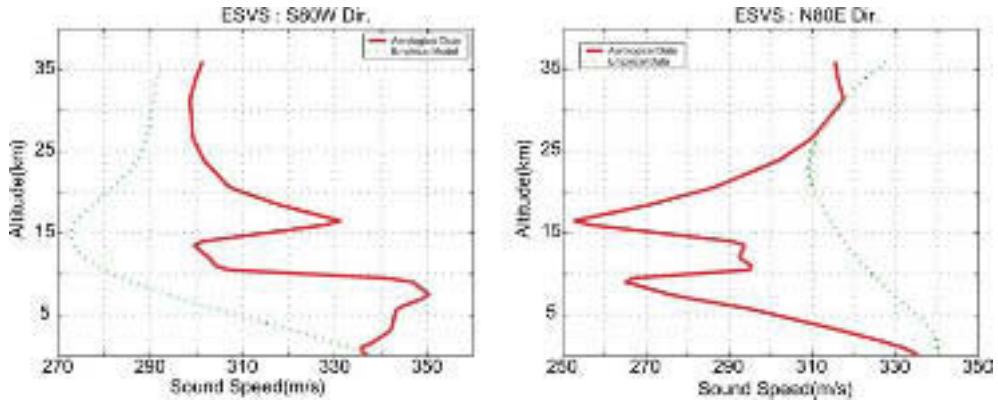

Figure 9. The figure shows a comparison of ESVS model for October in Korea (dotted line) with velocity model developed from meteorological observations in the troposphere. The left figure is for direction S80W and the right figure is for N80E.

Figure 9 compares the average October troposphere model with a model modified by local meteorological observations in October at Osan, Republic of Korea. The strong effect of low altitude winds is illustrated with ray tracing through the troposphere in the modified model (Figure 10). The velocity increase below 8 km for the S80W path provides a duct for the infrasound arrivals from 50 to 250 km away. Such troposphere ducting may result in the reported infrasound observations. This illustrates the importance of using local meteorological data during infrasound interpretation.

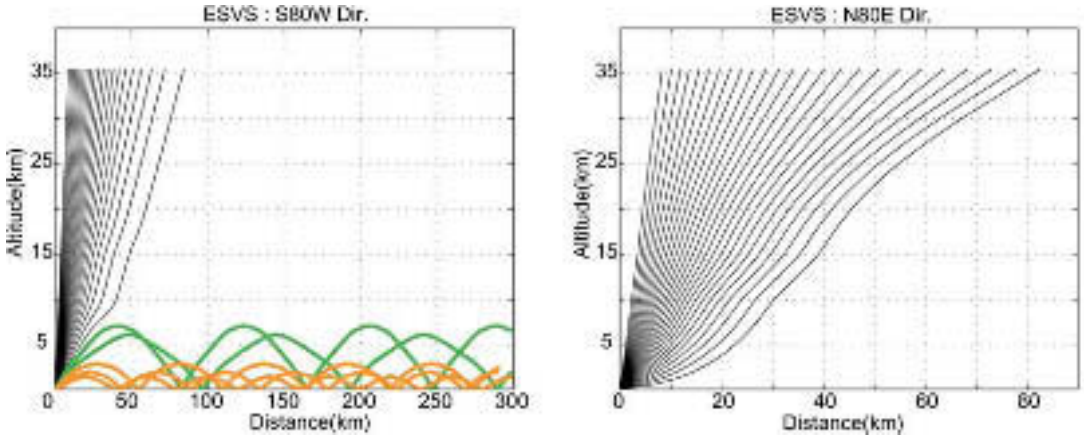

Figure 10. Plots show ray tracing through troposphere model based upon meteorological data. The left figure is for S80W and right figure is for N80E.

Characterizing Source Type

Seismic

Combining seismic and infrasound data can provide improved event characterization and identification. Regional seismic signatures indicative of a shallow explosive source include observations of strong high frequency P wave energy relative to L_g (Hartse et al., 1997) and short period R_g energy although regional attenuation along the propagation path can also affect P to L_g ratios and the R_g propagation degrades beyond 100-200 km . The preliminary data (Figure 4) provides an assessment of these propagation path effects. Figure 11 compares high frequency 8-10 Hz data from Event 7, an earthquake from the far southern tip of Korea and Event 4, an event from the north with an associated infrasound signal (Table 1). For event 4, R_g is observed at close stations such as CHNAR. For event 4, the P energy is dominant while for event 7 L_g dominates over P.

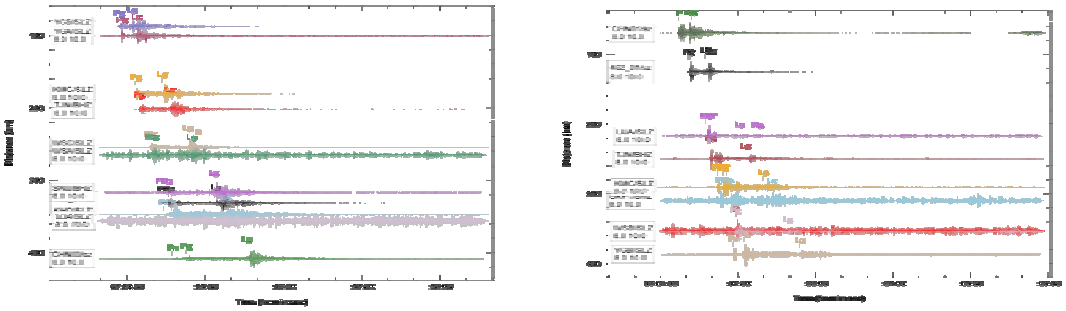

Figure 11: The left record section shows bandpass-filtered seismograms (8-10 Hz) from Event 7 (earthquake) and the right shows Event 4 (explosion based on accompanying infrasound signal).

Based on the network data reproduced in Figure 11, the relationship between P and L_g energy is insensitive to range. Detailed studies of the network data provide additional constraints on the regional Q structure across the Korean peninsula and a more detailed physical assessment of the contribution of propagation path effects to the regional phases.

Ground truth data provide the opportunity to further investigate the characteristics of seismic and acoustic signals and relate them to the source. A cluster of seismo-acoustic events 100 km to the SW of CHNAR was identified (Figure 1) and associated with the construction of Seoul s new Inchon International Airport. Overhead imagery of the construction site is included in Figure 1. Video images of the construction explosion indicate that besides the main blast designed to fracture the material for removal, additional nearly unstemmed explosives may be used to break individual rocks too large to remove mechanically. These additional blasts may radiate significant infrasound energy. The total blast duration is about 300 ms. Ground truth information, including some near-source seismic records, have been obtained from five mining and construction operations across the Republic of Korea. This information is used to assess the source size and characteristics and the associated seismic and infrasound signals. No explosions in this set exceed 3000 kg and many are much smaller, consistent with the small size of seismic signals reported for many of the seismo-acoustic events in Stump et al., 2000. A short event duration, 300 ms for the event at Inchon International Airport, is consistent with a small size explosive.

CONCLUSIONS AND RECOMMENDATIONS

1. Infrasound noise at CHNAR is strongly dependent upon near-surface wind velocity but seismic noise is almost independent of observed wind velocity.
2. The frequency locations of the amplitude peaks are the same for both microbaroms and microseisms.
3. In and around the Korean Peninsula, regional earthquakes and explosions are observed well beyond 400 km and can provide the basis for separating propagation and source effects at regional distances. Energy in excess of 8 Hz from these small events is efficiently transmitted along these propagation paths.
4. KIGAM broadband network data provides data for travel time analysis and waveform modeling. A preliminary velocity model has been developed from this data with Pn, Pg and Lg velocities of 8.2, 6.6 and 3.8 km/s. A modified single array location procedure is proposed based upon this preliminary model.
5. Infrasound signal travel paths in the 30 to 200 km range can be explained by local tropospheric winds and therefore local metrological must be included in the models.
6. There are nearly ten times more acoustic signals observed at CHNAR than seismic. Analysis of selected time windows over one year suggests that signal source location changes with time. Repeated signals are observed over $< -5^{o}$ azimuth bands during certain times of the year.
7. Evidence exists for the efficient generation of high frequency P energy relative to Lg for explosions over a large range of source to receiver distances suggesting that propagation path effects are secondary to this source effect.
8. Ground truth on mining explosions suggests that the majority of industrial explosions are < 3000 kg and < 300 ms total duration consistent with small, high frequency regional signals.

REFERENCES

Che, Il-Young, J.-S. Jeon and M.-S. Jun (2000). Infrasound wave propagation characteristics in Korea.

Donn, W. L. and E. S. Posmentier (1966), Infrasonic waves for the marine storm of April 7, *J. Geophys. Res., 72,* 2053.

Garc s, M. A., R. A. Hansen and K. G. Lindquist (1998), Traveltimes for infrasonic waves propagating in a stratified atmosphere, *Geophys. J. Int., 135,* 255-263.

Hagerty, M.T., W.-Y. Kim and P. Martysewvich (1999). Characteristics of Infrasound Produced by Large Mining Explosions in Kazakhstan, in Proceedings of the 21st Annual Seismic Research Symposium on Monitoring A Comprehensive Test Ban Treaty, 21-24 September 1999.

Hartse, H.E., S.R. Taylor, W.S. Phillips and G.E. Randall (1997). Preliminary Study of Seismic Discrimination in Central Asia with Emphasis on Western China, *Bull. Seism. Soc. Am., 87,* 1464-1474.

Jun, M.-S., J.-S. Jeon and I.-Y. Che (1999). Earthquake Mechanism of Korean Peninsula, *in preparation.*

Jun, M.-S. (1991). Body-Wave Analysis for Shallow Intraplate Earthquakes in the Korean Peninsula and Yellow Sea, *Tectonophysics, 192,* 345-357.

Jun, M.-S. and O. Kulhane (1991). Source Parameters of Earthquakes In and Around the Korean Peninsula Deduced from Spectral Analysis, *Physics of the Earth and Planetary Interiors, 65*, 255-266.

Kim, S. J. and S. G. Kim (1983), A study on the Crustal Structure of South Korea by using Seismic Waves, Jour. Korean Inst. Mining Geol., Vol. 16, NO. 1, P. 51-61.

Kim, S. K. and B. H. Jung, (1985), Crustal Structure of the Southern Part of Korea, Jour. Korean Inst. Mining Geol., Vol. 18, NO. 2, P. 151-157.

Kim, S. K. (1995), A study on the Crustal Structure of the Korean Peninsula, The Journal of the Geological Society of Korea, Vol. 31, No.4, p. 393-403.

Kim, S.G. and S. K. Lee (1997), Determination of Lateral Variations for Pn Velocity Structure Beneath the Korean Peninsula Using Seismic Tomography, Econ. Environ. Geol., Vol. 30, No. 6, p. 625-635.

Kim, S. G. and Z. Wu (1997). Uncertainties of Seismic Source Determination Using a 3-Component Single Station, *J. Phys. Earth, 45,* 1-11.

Kim, S.G. and Q. Li (1998), 3-D Crustal Velocity Tomography in the Southern Part of The Korean Peninsula, Econ. Environ. Geol., Vol. 31, No. 2, p. 127-139.

Kim, S.G. and Q. Li. (1998), 3-D Crustal Velocity Tomography in the Central Korean Peninsula, Econ. Environ. Geol., Vol. 31, No. 3, p. 235-247.

Kim, W. Y., D. W. Simpson, and P. G. Richards (1994). High-frequency spectra of regional phases from earthquakes and chemical explosions, , *Bull. Seism. Soc. Am., 84,* 1365-1386.

Lee, K (1979), On Crustal Structure of the Korean Peninsula, The Journal of the Geological Society of Korea, Vol. 15, No.4, p. 253-258.

McKisic, J. Michael (1997). Infrasound and the Infrasonic Monitoring of Atmospheric Nuclear Explosions: A Literature Review, Phillips Laboratory Technical Report, PL-TR-97-2123, 28 February 1997, Phillips Laboratory, Hanscom AFB, MA 01731-3010

Stump, B., C. Hayward, S.M. House, M.-S. Jun and J.-S. Jeon, 2000. A Small Aperture Seismo-Acoustic Array, Signals Assessment, in Proceedings of the 22nd Annual Seismic Research Symposium in Monitoring A Comprehensive Test Ban Treaty, September 2000, New Orleans, LA.